Comparative study of scattered electromagnetic waves from metamaterial coated cylinders

A. ILLAHI[a], A. GHAFFAR[b], M. M. ALI[c], Khalid A. IBRAHIM[d,e], N. M. ABDEL-SALAM[f], S. AHMED[g]
[a]*Research in Modeling and Simulation (RIMS) Group, Department of Physics, COMSATS Institute of Information Technology, Islamabad, Pakistan*
[b]*Department of Physics, University of Agriculture, Faisalabad, Pakistan*
[c]*Department of Physics, Allama Iqbal Open University, Islamabad, Pakistan*
[d]*College of Engineering, Muzahimiyah Branch, King Saud University, P.O.Box 2454. Riyadh 11451. Saudi Arabia*
[e]*Department of Chemical Engineering, Faculty of Engineering, Al-Hussein Bin Talal University, Ma'an, Jordan*
[f]*Arriyadh Community College, King Saud University, Arriyadh , Saudi Arabia*
[g]*Department of Electronics, Quaid-i-Azam University, Islamabad, Pakistan*

The behavior of electromagnetic wave scattering from coated cylinders of different materials is analyzed. Lengths of cylinders are infinite and coating is taken as uniform. Topological insulator cylinder coated with chiral, nihility cylinder coated with topological insulator, dielectric cylinder coated with topological insulator is considered for the analysis. Boundary value problem approach is used. Validation of formulation is confirmed by comparing numerical results with the available literature.

(Received August 16, 2016; accepted April 6, 2017)

Keywords: Dielectric, Chiral, Nihility, Topological insulator, Cylinders

1. Introduction

Controlling the back scattering echo-width of conducting objects is an important problem in antenna and radar applications. Coating a conductor by one or more layers of dielectric material affects the back scattering echo-width. Extensive literature on this topic is available. This includes scattering properties of EM waves in multilayered cylinder filled with double negative and positive materials [1], scattering from plasma coated PEMC cylinder placed in chiral metamaterial [1], dissipative and dispersive DNG materials, fractional dual interface in chiral nihility medium, chiral coated nihility cylinder [2], chiral cylinder placed in chiral metamaterial and Topological insulator [3-5]. Chiral medium is different from conducting and dielectric mediums as it generates both co- and cross- polarized scattered fields while interacting with electromagnetic waves. The lateral shifts from a slab of lossy chiral metamaterial have been predicted for both perpendicular and parallel components of the reflected fields in [6]. In chiral material the fields split into left circularly polarized and right circularly polarized waves which propagate with different phase velocities. The field with the latter polarization travelling through right handed medium is faster than the left circularly polarized wave and vice versa. This property of chiral mediums is called handedness. Selected work in electromagnetic [7] chirality includes: shift at the surface of chiral negative refractive media, chiral nihility effects on energy flow in chiral materials [8]. Other multi layered chiral cylinders are treated by M. S. Kuleskens and E. H. Newman [9, 10]. Engheta and Bassiri gave the solutions for one and two-dimensional dyadic Greens functions in chiral media [11]. Lakhtakia et al. explained the field equations, Huygens principle, integral equations, and theorems for radiation and scattering of electromagnetic waves in isotropic chiral media [12]. Electromagnetic chirality and its applications have been discussed by Engheta and Jaggard [13]. Al-Kanhal and Arvas presented simple integral equation and MoM solution to the problem of TE and TM scattering from a lossy homogeneous chiral cylinder of arbitrary cross-section [14]. C. Li and Z. Shen discussed the scattering from metamaterial coated cylinders [15]. Buried simple cylinder is discussed in [16]. Topological insulator circular cylinder buried in semi-infinite medium and slightly rough surface has been analyzed in [17-19] respectively. Besides scattering from simple cylinder of different materials, a lot of work has been done on scattering from coated cylinders with different materials.

In 1959 Fedorov and Bokut improved the Born's proposal of chirality and gave the following equation/constitutive relations [20]:

$$\boldsymbol{D} = \in [\boldsymbol{E} + \beta \nabla \times \boldsymbol{E}] \quad (1)$$

$$\boldsymbol{B} = \mu [\boldsymbol{H} + \beta \nabla \times \boldsymbol{H}] \quad (2)$$

β in the above equation is the chirality parameter having a unit of length. Above relations are also known as Drude-Born-Fedorov constitutive relations. We will use these relations in our analysis.

Nihility medium introduced by Lakhtakia drew the attention of many researchers [21]. Nihility is a special type of medium in which both relative permittivity and permeability are null-valued [22]. So the Maxwell equations reduce to

$$\nabla \times \boldsymbol{H} = 0 \quad (3)$$

$$\nabla \times \boldsymbol{E} = 0 \quad (4)$$

Topological insulator is such type of material which behaves as an insulator in its interior but its surface contains conducting states. The constitutive relations of topological insulators in SI units are [23]

$$\boldsymbol{D} = \epsilon_0 \epsilon_r \boldsymbol{E} - \epsilon_0 \alpha \frac{\theta}{\pi}(c_0 \boldsymbol{B}) \quad (5)$$

$$c_0 \boldsymbol{H} = \frac{c_0 \boldsymbol{B}}{\mu} + \alpha \frac{\theta}{\pi} \frac{\boldsymbol{E}}{\mu_0} \quad (6)$$

where α is fine structure constant and θ is quantized and takes integer multiples of π for topological non trivial materials otherwise zero. c_0 is the speed of light in vacuum [24]. In the present work analytical solutions are derived for the scattering of an electromagnetic plane wave from coated circular cylinders. Both cylinder and the coating layer are infinite along the cylindrical axis. Parallel polarization is considered for analysis. The response for the coated geometry has been observed. The numerical results are compared with the published literature and are found in good agreement.

2. Formulations

In Fig. 1, electromagnetic plane wave is incident normally on a coated circular cylinder of infinite length, having radius "a" of cylinder and thickness "b-a" of coating is placed in free space. The region outside the coating $\rho > b$ is a free space and its wave number is $k_0 = \omega\sqrt{\mu_0 \epsilon_0}$ and permittivity and permeability ϵ_0 and μ_0 mentioned as region I, the region $a < \rho < b$ is termed as region II having medium I and the region $\rho < a$ is termed as region III having medium II. Incident wave is TM polarized and electric field vector is parallel to the axis of cylinder. Time dependency is taken as $e^{-i\omega t}$. Radii *"a"* and *"b"* are taken in the units of λ.

Case I: Topological Insulator Cylinder Coated with Chiral/chiral-nihility Material

The geometry of problem is shown in Fig. 1, in this case medium I is chiral having wave numbers as $k_L = \frac{\omega\sqrt{\mu_c \epsilon_c}}{1-\beta\omega\sqrt{\mu_c \epsilon_c}}$ and $k_R = \frac{\omega\sqrt{\mu_c \epsilon_c}}{1+\beta\omega\sqrt{\mu_c \epsilon_c}}$. ϵ_c, μ_c, ξ and β are permittivity, permeability, chiral admittance and chirality parameter (cp) respectively. Medium II is topological insulator having wave number $k_T = \omega\sqrt{\mu_T \epsilon_T}$. ϵ_T and μ_T are permittivity, permeability for topological insulator medium respectively.Where $\mu_c = \mu_0 \mu_{rc}$, $\epsilon_c = \epsilon_0 \epsilon_{rc}$, with ϵ_{rc} and μ_{rc} are the relative permittivity of chiral medium.

Incident fields in region I are as follows

$$E^{inc} = \frac{1}{k_0} \sum_{n=-\infty}^{\infty} k_0 i^n J_n(k_0 \rho)\, e^{in\phi} \hat{z} \quad (7)$$

$$B^{inc} = \frac{1}{i\omega} \sum_{n=-\infty}^{\infty} i^n \left(\frac{in}{\rho} J_n(k_0 \rho) e^{in\phi} \hat{\rho} - k_0 J_n'(k_0 \rho)\, e^{in\phi} \hat{\phi} \right) \quad (8)$$

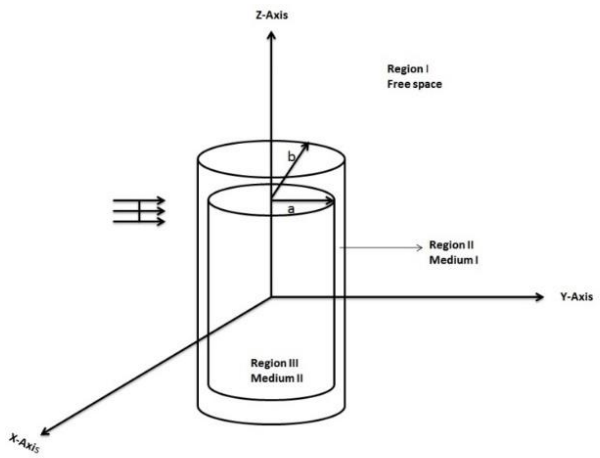

Fig. 1 Geometry of Coated Cylinder

Similarly scattered fields in region I are as follows [9].

$$E^{sca} = \frac{-1}{k_0} \sum_{n=-\infty}^{\infty} i^n \Big(a_n k_0 H_n^{(1)}(k_0 \rho)\, e^{in\phi} \hat{z} + i\, b_n \big(\frac{in}{\rho} H_n^{(1)}(k_0 \rho) e^{in\phi} \hat{\rho} - k_0 H_n'^{(1)}(k_0 \rho)\, e^{in\phi} \hat{\phi} \big) \Big) \quad (9)$$

$$B^{sca} = \frac{-1}{i\omega} \sum_{n=-\infty}^{\infty} i^n \left(a_n \left(\frac{in}{\rho} H_n^{(1)}(k_0 \rho) e^{in\phi} \hat{\rho} - k_0 H_n'^{(1)}(k_0 \rho)\, e^{in\phi} \hat{\phi} \right) + i b_n k_0 H_n^{(1)}(k_0 \rho)\, e^{in\phi} \hat{z} \right) \quad (10)$$

The fields in region II which is chiral are given as

$$E_z^c = \frac{1}{k_0} \sum_{n=-\infty}^{\infty} i^n \big(c_n k_L J_n(k_L \rho)\, e^{in\phi} - a_R d_n k_R J_n(k_R \rho)\, e^{in\phi} + e_n k_L H_n^{(1)}(k_L \rho)\, e^{in\phi} - a_R f_n k_R H_n^{(1)}(k_R \rho)\, e^{in\phi} \big) \quad (11)$$

$$B_\phi^c = \frac{-1}{i\omega} \sum_{n=-\infty}^{\infty} i^n \big(a_L c_n k_L J_n'(k_L \rho)\, e^{in\phi} + d_n k_R J_n'(k_R \rho)\, e^{in\phi} + a_L e_n k_L H_n'^{(1)}(k_L \rho)\, e^{in\phi} + f_n k_R H_n'^{(1)}(k_R \rho)\, e^{in\phi} \big) \quad (12)$$

$$B_z^c = \frac{1}{i\omega}\sum_{n=-\infty}^{\infty} i^n\big(a_L c_n k_L J_n(k_L\rho)\, e^{in\phi} - d_n k_R J_n(k_R\rho)\, e^{in\phi} + a_L e_n k_L H_n^{(1)}(k_L\rho)\, e^{in\phi} - f_n k_R H_n^{(1)}(k_R\rho)\, e^{in\phi}\big) \quad (13)$$

$$E_\phi^c = -\frac{1}{k_0}\sum_{n=-\infty}^{\infty} i^n\big(c_n k_L J_n'(k_L\rho)\, e^{in\phi} + a_R d_n k_R J_n'(k_R\rho)\, e^{in\phi} + e_n k_L H_n'^{(1)}(k_L\rho)\, e^{in\phi} + a_R f_n k_R H_n'^{(1)}(k_R\rho)\, e^{in\phi}\big) \quad (14)$$

Region III which is Topological insulator, the fields in this region are

$$E^T = R_L + a_R R_R \quad (15)$$
$$H^T = R_R + a_L R_L \quad (16)$$

k_L and k_R are in case of TI is equal to k_T

where $a_L = -i\sqrt{\frac{\epsilon_r}{\mu_r}}$, $a_R = -i\sqrt{\frac{\mu_r}{\epsilon_r}}$, R_L and R_R are left and right circular polarized waves.

$$E_z^T = \frac{1}{k_0}\sum_{n=-\infty}^{\infty} i^n\big(g_n k_T J_n(k_T\rho)\, e^{in\phi} - a_R h_n k_T J_n(k_T\rho)\, e^{in\phi}\big) \quad (17)$$

$$B_\phi^T = \frac{-1}{i\omega}\sum_{n=-\infty}^{\infty} i^n\big(a_L g_n k_T J_n'(k_T\rho)\, e^{in\phi} + h_n k_T J_n'(k_T\rho)\, e^{in\phi}\big) \quad (18)$$

$$B_z^T = \frac{1}{i\omega}\sum_{n=-\infty}^{\infty} i^n\big(a_L g_n k_T J_n(k_T\rho)\, e^{in\phi} - h_n k_T J_n(k_T\rho)\, e^{in\phi}\big) \quad (19)$$

$$E_\phi^T = -\frac{1}{k_0}\sum_{n=-\infty}^{\infty} i^n\big(g_n k_T J_n'(k_T\rho)\, e^{in\phi} + a_R h_n k_T J_n'(k_T\rho)\, e^{in\phi}\big) \quad (20)$$

Now apply following boundary conditions at interfaces

At $\rho = b$

$$E_z^{inc} + E_z^{sca} = E_z^c \quad (21)$$
$$H_\phi^{inc} + H_\phi^{sca} = H_\phi^c \quad (22)$$
$$H_z^{sca} = H_z^c \quad (23)$$
$$E_\phi^{sca} = E_\phi^c \quad (24)$$

At $\rho = a$

$$E_z^c = E_z^T \quad (25)$$
$$\frac{1}{\mu_c}B_\phi^c = \frac{1}{\mu_T}B_\phi^T + \frac{\alpha\theta}{c_0\pi}\frac{1}{\mu_0}E_\phi^T \quad (26)$$
$$\frac{1}{\mu_c}B_Z^c = \frac{1}{\mu_T}B_Z^T + \frac{\alpha\theta}{c_0\pi}\frac{1}{\mu_0}E_z^T \quad (27)$$
$$E_\phi^c = E_\phi^T \quad (28)$$

By solving above equations unknowns can be obtained and used to plot echo widths as given in equations

$$\frac{\sigma_{co}}{\lambda_0} = \frac{2}{\pi}\left|\sum_{n=-\infty}^{\infty} a_n e^{in(\phi)}\right|^2 \quad (29)$$
$$\frac{\sigma_{cross}}{\lambda_0} = \frac{4}{\pi}\left|\sum_{n=-\infty}^{\infty} b_n e^{in(\phi)}\right|^2 \quad (30)$$

All infinite series are truncated after n_{max} term. For this number J. J. Bowman [25] proposed the value $n_{max} = (\frac{1}{2}ka)^{\frac{1}{3}}$, where ka is the size parameter of the cylinder, and this value is used here.

3. Numerical results and discussions

Figs. 2 and 3 results are obtained for topological insulator cylinder coated with chiral layer. Radius of cylinder and coating is taken as 0.63 and 1.26 respectively. Relative permeability and relative permittivity of cylinder are taken as 1 and 100 respectively, while for coating is 2 and 4 respectively. Figs. 4 and 5 show the comparison in which the radius of the cylinder is taken as zero while radius of coating is reduced to 0.1. Relative permeability and relative permittivity are taken as 4 and 1.5 respectively. Obtained results are in good agreement with the published results. Figs. 6 and 7 show the scattering behavior of topological insulator cylinder coated with chiral nihility material. Radius for cylinder and coating are taken as 0.63 and 1.26 respectively. Figs. 8 and 9 show the comparison of topological insulator cylinder coated chiral nihility medium with simple topological insulator cylinder.

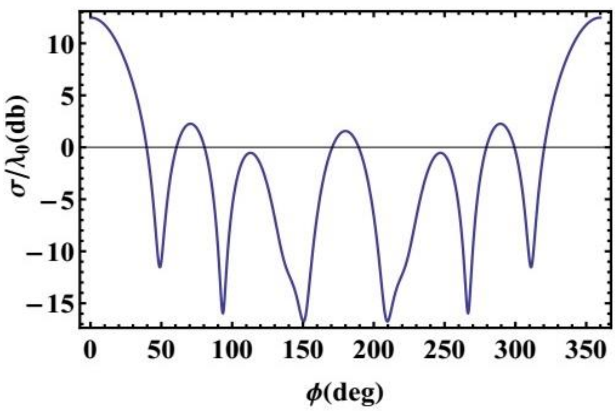

Fig. 2. Co-Polarized component of bi-static echo width of Chiral coated TI cylinder in free space with $\boldsymbol{a = 0.63\lambda, b = 1.26\lambda, \mu_{rc} = 2, \epsilon_{rc} = 4, \mu_{rT} = 1, \mu_{rT} = 100, \alpha = \frac{1}{4\pi\epsilon_0}\frac{e^2}{\hbar c_0}, cp = \frac{0.15}{k0}}$ ***and*** $\boldsymbol{\theta = 41\pi}$.

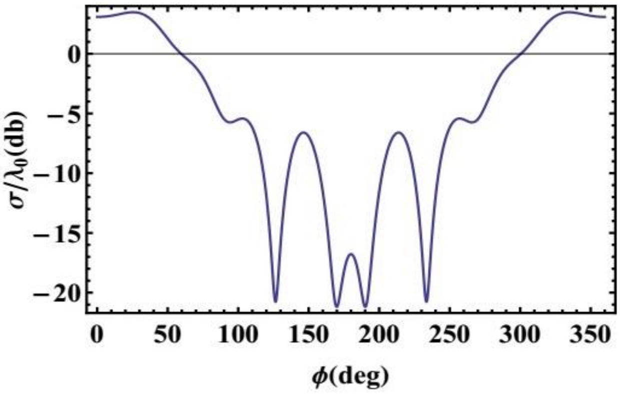

Fig. 3. Cross-Polarized component of bi-static echo width of Chiral coated TI cylinder in free space with $\boldsymbol{a = 0.63\lambda, b = 1.26\lambda, \mu_{rc} = 2, \epsilon_{rc} = 4, \mu_{rT} = 1, \mu_{rT} = 100, \alpha = \frac{1}{4\pi\epsilon_0}\frac{e^2}{\hbar c_0}, cp = \frac{0.15}{k0}}$ ***and*** $\boldsymbol{\theta = 41\pi}$.

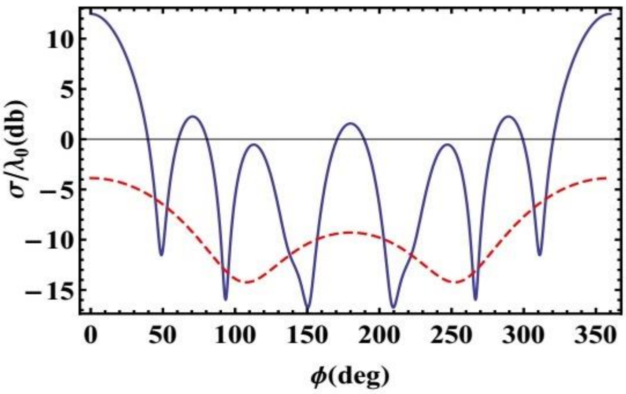

Fig. 4. Comparison of chiral coated TI cylinder co-polarized with [26] only Co-Polarized component solid line with $a = 0.63\lambda, b = 1.26\lambda, \mu_{rc} = 2, \epsilon_{rc} = 4, \mu_{rT} = 1, \epsilon_{rT} = 100$ *and dashed line with* $a = 0, b = 0.1\lambda, \mu_{rc} = 4, \epsilon_{rc} = 1.5, \mu_{rT} = 1, \epsilon_{rT} = 100$.

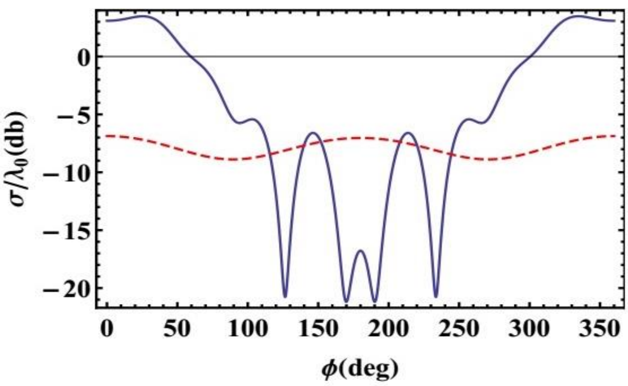

Fig. 5. Comparison of chiral coated TI cylinder cross-polarized with [26] only Cross-Polarized component with solid line $\boldsymbol{a = 0.63\lambda, b = 1.26\lambda, \mu_{rc} = 2, \epsilon_{rc} = 4, \mu_{rT} = 1, \epsilon_{rT} = 4}$ ***and dashed line with*** $\boldsymbol{a = 0, b = 0.1\lambda, \mu_{rc} = 4, \epsilon_{rc} = 1.5, \mu_{rT} = 1, \epsilon_{rT} = 100}$.

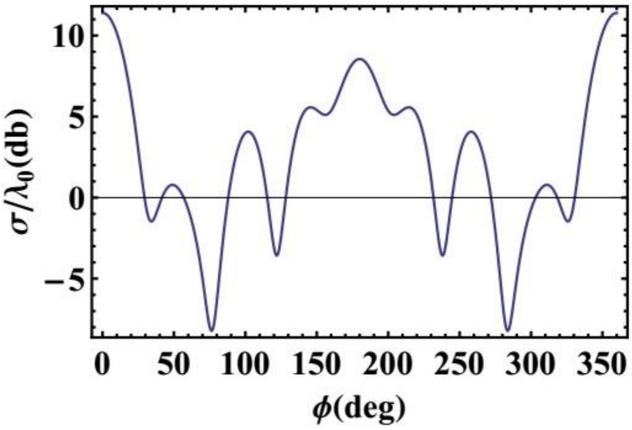

Fig. 6. Co-polarized component of bi-static echo width of chiral-nihility coated Topological insulator circular cylinder with $a = 0.63\lambda, b = 1.26\lambda, \mu_{rc} = 10^{-5}, \epsilon_{rc} = 10^{-5}, \mu_{rT} = 1, \epsilon_{rT} = 100, \alpha = \frac{1}{4\pi\epsilon_0}\frac{e^2}{\hbar c_0}, cp = \frac{0.15}{k0}$ *and* $\theta = 41\pi$

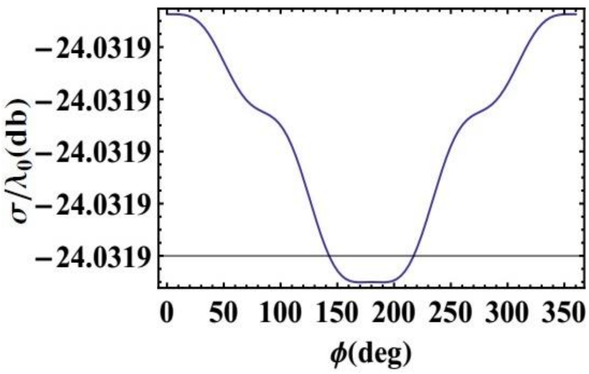

Fig. 7. Cross-polarized component of bi-static echo width of chiral-nihility coated Topological insulator circular cylinder with $\boldsymbol{a = 0.63\lambda, b = 1.26\lambda, \mu_{rc} = 10^{-5}, \epsilon_{rc} = 10^{-5}, \mu_{rT} = 1, \epsilon_{rT} = 100, \alpha = \frac{1}{4\pi\epsilon_0}\frac{e^2}{\hbar c_0}, cp = \frac{0.15}{k0}}$ ***and*** $\boldsymbol{\theta = 41\pi}$.

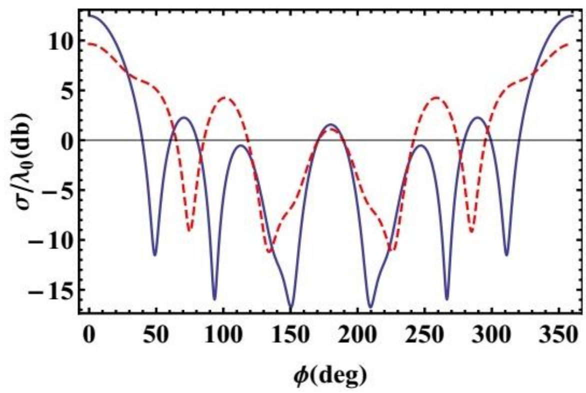

Fig. 8. Comparison of Chiral coated TI cylinder with simple TI cylinder Co-Polarized component solid line with $\boldsymbol{a = 0.63\lambda, b = 1.26\lambda, \mu_{rc} = 2, \epsilon_{rc} = 4, \mu_{rT} = 1, \epsilon_{rT} = 100}$ *and dashed line with* $\boldsymbol{a = 0.63\lambda, b = 0.63\lambda, \mu_{rc} = 2, \epsilon_{rc} = 4, \mu_{rT} = 1, \epsilon_{rT} = 100}$.

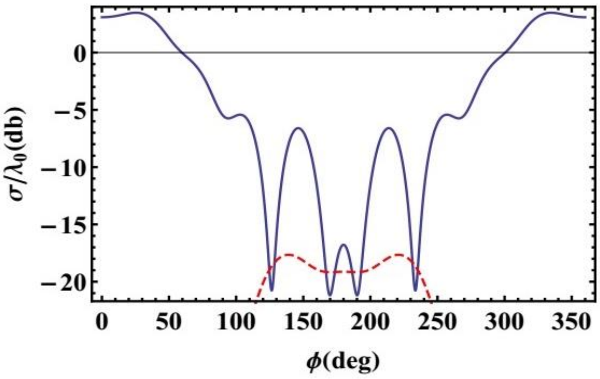

Fig. 9. Comparison of chiral coated TI with simple TI cylinder Cross-Polarized component solid line with $\boldsymbol{a = 0.63\lambda, b = 1.26\lambda, \mu_{rc} = 2, \epsilon_{rc} = 4, \mu_{rT} = 1, \epsilon_{rT} = 100}$ *and dashed line with* $\boldsymbol{a = 0.63\lambda, b = 0.63\lambda, \mu_{rc} = 2, \epsilon_{rc} = 4, \mu_{rT} = 1, \epsilon_{rT} = 100}$.

Case II: Nihility Cylinder Coated with Topological Insulator Material

Fig. 1 shows the geometry in which Circular cylinder of nihility material is coated with topological insulator of uniform thickness. The cylinder is supposed to be of infinite length. Radius of nihility cylinder is $"a"$ while with coating of topological insulating layer is $"b-a"$. The region (region I) outside the coating $\rho > b$ is a free space and its wave number is $k_0 = \omega\sqrt{\mu_0\epsilon_0}$. For this case medium I is topological insulator, the wave number for this region is $k_T = \omega\sqrt{\mu_T\epsilon_T}$, while the medium II is nihility cylinder termed as region III the wave number for this region is $k_n = \omega\sqrt{\mu_n\epsilon_n}$, $\mu_n = \mu_0\mu_{rn}$, μ_{rn} is relative permeability of nihility medium and $\epsilon_n = \epsilon_0\epsilon_{rn}$, ϵ_{rn} is relative permittivity of nihility medium

Incident fields in region I are as follows

$$E_z^{inc} = E_0 \sum_{n=-\infty}^{\infty} i^n J_n(k_0\rho)\, e^{in\phi} \tag{31}$$

Using Maxwell equations ϕ-component of magnetic field can be written as

$$B_\phi^{inc} = i\sqrt{\mu_0\epsilon_0}E_0 \sum_{n=-\infty}^{\infty} i^n J_n'(k_0\rho)\, e^{in\phi} \tag{32}$$

Similarly the scattered fields in region I are

$$E_z^{sca} = E_0 \sum_{n=-\infty}^{\infty} i^n a_n H_n^{(1)}(k_0\rho)\, e^{in\phi} \tag{33}$$

$$B_\phi^{sca} = i\sqrt{\mu_0\epsilon_0}E_0 \sum_{n=-\infty}^{\infty} i^n a_n H_n'^{(1)}(k_0\rho)\, e^{in\phi} \tag{34}$$

$$B_z^{sca} = -i\sqrt{\mu_0\epsilon_0}E_0 \sum_{n=-\infty}^{\infty} i^n b_n H_n^{(1)}(k_0\rho)\, e^{in\phi} \tag{35}$$

$$E_\phi^{sca} = -E_0 \sum_{n=-\infty}^{\infty} i^n b_n H_n'^{(1)}(k_0\rho)\, e^{in\phi} \tag{36}$$

Now applying following boundary conditions at $\rho = b$, we have

$$E_z^{inc} + E_z^{sca} = E_z^T \tag{37}$$

$$\frac{1}{\mu_0}B_\phi^{inc} + \frac{1}{\mu_0}B_\phi^{sca} = \frac{1}{\mu_T}B_\phi^T + \frac{\alpha\theta}{C_0\pi}\frac{1}{\mu_0}E_\phi^T \tag{38}$$

$$\frac{1}{\mu_0}B_z^{sca} = \frac{1}{\mu_T}B_z^T + \frac{\alpha\theta}{C_0\pi}\frac{1}{\mu_0}E_z^T \tag{39}$$

$$E_\phi^{sca} = E_\phi^T \tag{40}$$

At $\rho = a$

$$E_z^T = E_z^n \tag{41}$$

$$\frac{1}{\mu_T}B_\phi^T + \frac{\alpha\theta}{C_0\pi}\frac{1}{\mu_0}E_\phi^T = \frac{1}{\mu_n}B_\phi^n \tag{42}$$

$$\frac{1}{\mu_T}B_z^T + \frac{\alpha\theta}{C_0\pi}\frac{1}{\mu_0}E_z^T = \frac{1}{\mu_n}B_z^n \tag{43}$$

$$E_\phi^T = E_\phi^n \tag{44}$$

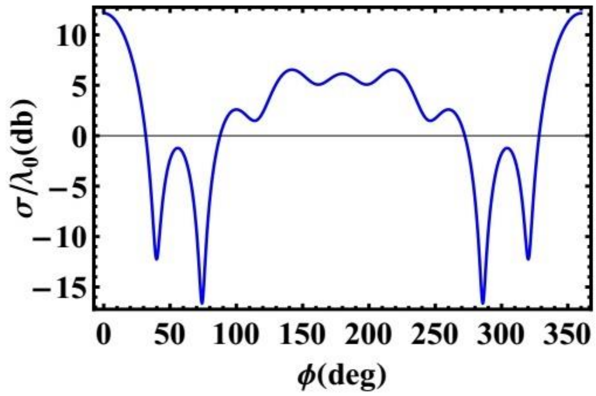

Fig. 10. The co-polarized echo width for topological insulator coated nihility cylinder, TM case with $\boldsymbol{a = 0.63\lambda, b = 1.26\lambda, \mu_{rn} = 10^{-5}, \epsilon_{rn} = 10^{-5}, \mu_{rT} = 1, \epsilon_{rT} = 100, \alpha = \frac{1}{4\pi\epsilon_0}\frac{e^2}{\hbar c_0}, cp = \frac{0.15}{k0}}$ ***and*** $\boldsymbol{\theta = 41\pi}$.

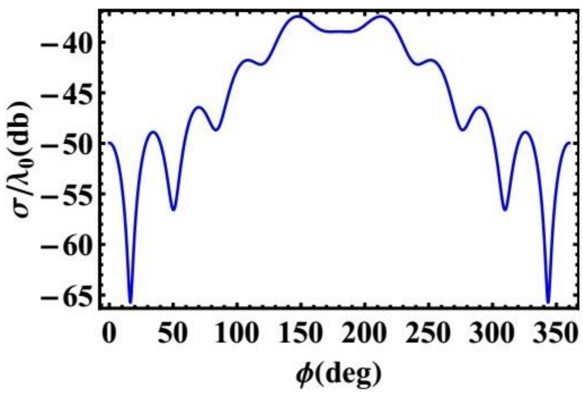

Fig. 11. The cross-polarized echo width for topological insulator coated nihility cylinder, TM case with $\boldsymbol{a = 0.63\lambda, b = 1.26\lambda, \mu_{rn} = 10^{-5}, \epsilon_{rn} = 10^{-5}, \mu_{rT} = 1, \epsilon_{rT} = 100, \alpha = \frac{1}{4\pi\epsilon_0}\frac{e^2}{\hbar c_0}, cp = \frac{0.15}{k0}}$ ***and*** $\boldsymbol{\theta = 41\pi}$.

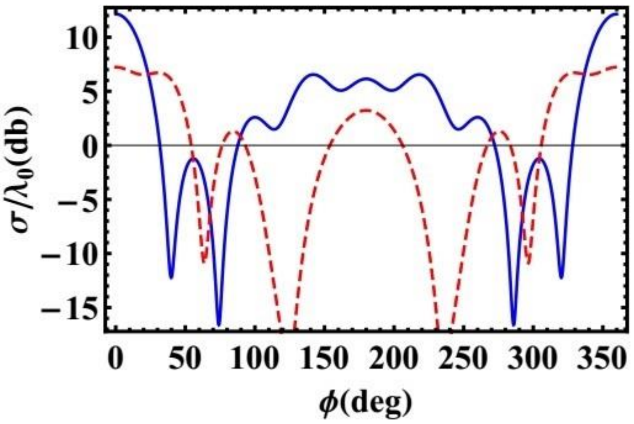

Fig. 12. Comparison of co-polarized echo widths for topological insulator coated nihility cylinder with simple dielectric cylinder solid line with $\boldsymbol{a = 0.63\lambda, 10^{-5}, b = 1.26\lambda, , \mu_{rT} = 1, \epsilon_{rT} = 4}$ *and dashed line with* $\boldsymbol{a = 0.63\lambda, b = 1.26\lambda, \mu_{rn} = 10^{-5}, \epsilon_{rn} = 10^{-5}, \mu_{rT} = 1, \epsilon_{rT} = 100}$.

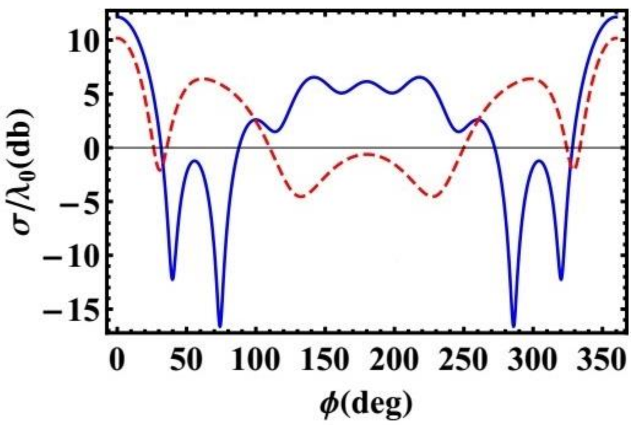

Fig. 13. Comparison of co-polarized echo widths for topological insulator coated nihility with simple nihility cylinder solid line with $\boldsymbol{a = 0.63\lambda, b = 1.26\lambda, \mu_{rT} = 10^{-5} \epsilon_{rT} = 10^{-5}}$ *and dashed line with* $\boldsymbol{a = 0.63\lambda, b = 0.63\lambda, \ \mu_{rT} = 1 \ \epsilon_{rT} = 100 \ and \ \theta = 41\pi}$.

Figs. 10 and 11 shows the results for nihility cylinder coated with topological insulator. Radius of cylinder is taken as 0.63 and that of coating is 1.26, relative permittivity and permeability for topological insulator medium is taken as 100 and 1 while for nihility cylinder are taken as 10^{-5} and 10^{-5}. Figs. 12 and 13 show the comparison of nihility cylinder coated with topological insulator with simple dielectric and simple nihility cylinder.

Case III: Dielectric Cylinder Coated with Topological Insulator Material

Fig. 1 shows the geometry in which circular cylinder of dielectric material is coated with topological insulator of uniform thickness. The cylinder is supposed to be of infinite length. Radius of dielectric cylinder is $"a"$ while with coating of topological insulating layer is $"b - a"$. The region outside the coating $\rho > b$ is a free space and its wave number is $k_0 = \omega\sqrt{\mu_0\epsilon_0}$ mentioned as region I. For this case medium I is topological insulator, the wave number for this region is $k_T = \omega\sqrt{\mu_T\epsilon_T}$, while the medium II is dielectric cylinder termed as region III the wave number for this region is $k_d = \omega\sqrt{\mu_d\epsilon_d}$, $\mu_d = \mu_0\mu_{rd}$, μ_{rd} is relative permeability of dielectric medium and $\epsilon_d = \epsilon_0\epsilon_{rd}$, ϵ_{rd} is relative permittivity of dielectric medium

Incident and scattered fields are same as discussed in case-II (31 to 36).Boundary conditions at the interface are as first four boundary conditions at $\rho = b$ are same as in equations 37 to 40

At $\rho = a$

$$E_z^T = E_z^D \tag{45}$$

$$\frac{1}{\mu_T}B_\phi^T + \frac{\alpha\theta}{C_0\pi}\frac{1}{\mu_0}E_\phi^T = \frac{1}{\mu_D}B_\phi^D \tag{46}$$

$$\frac{1}{\mu_T}B_z^T + \frac{\alpha\theta}{C_0\pi}\frac{1}{\mu_0}E_z^T = \frac{1}{\mu_D}B_z^D \tag{47}$$

$$E_\phi^T = E_\phi^D \tag{48}$$

By solving above equations unknowns can be obtained and used to plot echo widths as given in equations 29 and 30.

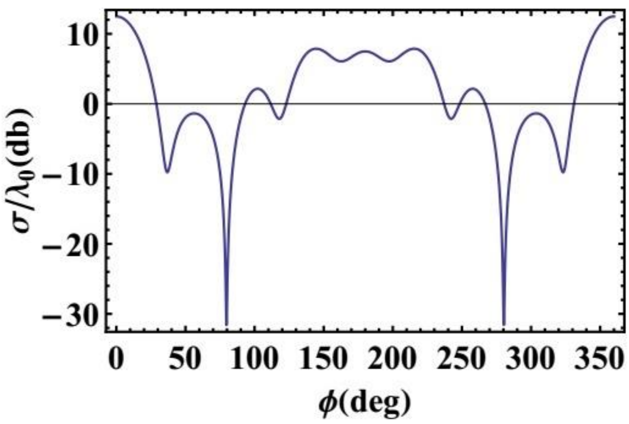

Fig. 14.The co-polarized echo width for long infinite dielectric cylinder coated with topological insulator, TM case with $\boldsymbol{a = 0.63\lambda, b = 1.26\lambda, \mu_{rd} = 1, \epsilon_{rd} = 4, \mu_{rT} = 1, \epsilon_{rT} = 100, \alpha = \frac{1}{4\pi\epsilon_0}\frac{e^2}{\hbar c_0} and \ \theta = 41\pi}$.

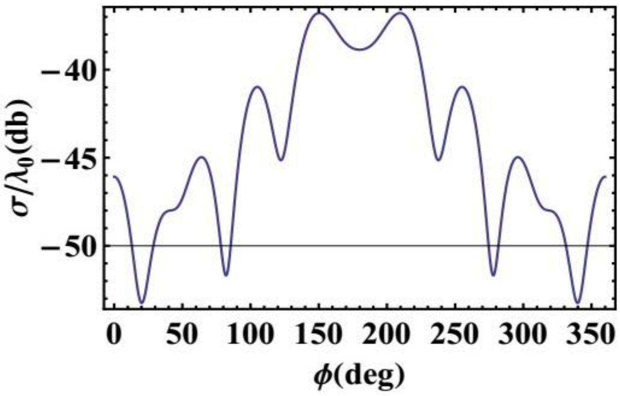

Fig. 15. The cross-polarized echo width for long infinite dielectric cylinder coated with topological insulator, TM case with $\boldsymbol{a = 0.63\lambda, b = 1.26\lambda, \mu_{rd} = 1, \epsilon_{rd} = 4, \mu_{rT} = 1, \epsilon_{rT} = 100, \alpha = \frac{1}{4\pi\epsilon_0}\frac{e^2}{\hbar c_0}}$ $\boldsymbol{and\ \theta = 41\pi}$

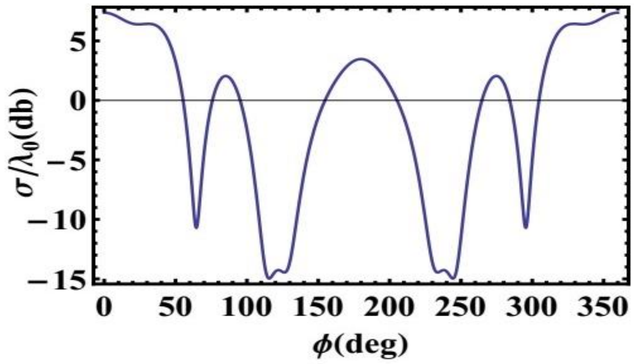

Fig. 16. Comparison of co-polarized echo width for long infinite dielectric cylinder coated with topological insulator with simple dielectric cylinder with $\boldsymbol{a = 10^{-5}\lambda, b = 0.63\lambda, \mu_{rd} = 1, \epsilon_{rd} = 4, \mu_{rT} = 1, \epsilon_{rT} = 100, \alpha = \frac{1}{4\pi\epsilon_0}\frac{e^2}{\hbar c_0}}$ $\boldsymbol{and\ \theta = 41\pi}$.

Figs. 14 and 15 show the results for the dielectric cylinder coated with topological insulator. For dielectric cylinder relative permittivity and relative permeability are taken as 1 and 4. Radius for the cylinder is taken as 0.63 and 1.26 respectively. Fig. 16 is the comparison of dielectric cylinder coated with topological insulator with simple dielectric cylinder.

4. Conclusion

From all the numerical results it can be observed that the obtained results are in good agreement with already published work. The fields can be maximized or minimized by changing the chirality parameter and thickness of coating layer. Co-polarized and cross-polarized echo widths can be controlled by changing the angle of incidence, the angle of observation, the radius of cylinder and constitutive parameters. This provides the designers to control the echo width of scatterer. In case of chiral, rapid variation in the field of the scattered wave with different scattering angles has been observed. So chirality of cylinder plays an important role in the control of RCS. In case of nihility and dielectric coated with topological insulter the echo-width approaches to zero. It is another striking result. The Metamaterials coating can also be used to decrease the echo-width of a conducting cylinder.

Acknowledgement

The authors would like to extend their sincere appreciation to The Deanship of Scientific Research (DSR) at King Saud University, Riyadh, Saudi Arabia for their financial support through the Research Group Project No. RG-1438-020.

References

[1] H. Y. Yao, L. W. Li, C. W. Qiu, Q. Wu, Z. N. Chen, Radio Science, **42**(2), (2007).
[2] M. Yaqoob, A. Ghaffar, M. A. Alkanhal, I. Shakir, Q. Naqvi, Optical Materials Express **5**, 1224 (2015).
[3] S. Ahmed, M. Naveed, A. Ghaffar, A. A. Syed, Q. Naqvi, Mathematical Problems in Engineering **2011**, 1 (2011).
[4] S. Ahmed, F. Manan, A. Shahzad, Q. A. Naqvi, Progress in Electromagnetics Research M **19**, 239 (2011).
[5] S. Ahmed, Q. A. Naqvi, Journal of Infrared, Millimeter, and Terahertz Waves **30**, 1044 (2009).
[6] H. Bin-Jie, E. Y. Kai-Ning, Z. Jun, T. Serge, Chinese Physics **14**, 2305 (2005).
[7] W. Dong, L. Gao, C.-W. Qiu, "Goos-HÄanchen shift at the surface of chiral negative refractive media," in Metamaterials, 2008 International Workshop on, 2008, pp. 77.
[8] C.-W. Qiu, N. Burokur, S. Zouhdi, L.-W. Li, J. Opt. Soc. Am. A **25**, 55 (2008).
[9] M. S. Kluskens, E. H. Newman, Antennas and Propagation, IEEE Transactions on **38**, 1448 (1990).
[10] D. M. Pozar, IEEE transactions on Antennas and Propagation **40**, 1260 (1992).
[11] N. Engheta, S. Bassiri, IEEE transactions on antennas and propagation **37**, 512 (1989).
[12] A. Lakhtakia, V. V. Varadan, V. K. Varadan, J. Opt. Soc. Am. A **5**, 175 (1988).
[13] N. Engheta, D. L. Jaggard, IEEE Antennas and Propagation Society Newsletter **30**, 6 (1988).
[14] M. A. Al-Kanhal, E. Arvas, IEEE Transactions on Antennas and Propagation **44**, 1041 (1996).
[15] C. L. Z. Shen, Progress in Electromagnetics Research **42**, 91 (2003).
[16] T. C. Rao, R. Barakat, JOSA A **6**, 1270 (1989).
[17] L. Zeng, R. Song, X. Jian, Modern Physics Letters B **27**, 1350098 (2013).
[18] M. Akhtar, N. A. Naz, M. Fiaz, Q. Naqvi, Journal of Modern Optics **61**, 697 (2014).
[19] X.-L. Qi, S.-C. Zhang, Reviews of Modern Physics **83**, 1057 (2011).

[20] A. H. S. I. V. Lindell, S. A. Tretyakov, A. J. Viitanen, Electromagnetic Waves in Chiral and Bi-isotropic Media, 1994.
[21] A. Lakhtakia, Int. J. Infrared Millim. Waves **23**, 813 (2002).
[22] A. Lakhtakia, Int. J. Infrared Millim. Waves **22**, 1731 (2001).
[23] A. Karch, Physical Review B **83**, 245 (2011).
[24] Xiao-Liang Qi, Shou-Cheng Zhang, Rev. Mod. Phys. **83**, 1057 (2011).
[25] J. J. Bowman, T. B. A. Seniour, P. L. E. Uslenghi. Electromagnetic and acoustic scattering by simple shapes, New York, Hemisphere Publishing Corp., 1987.
[26] M. A. Al-Kanhal, E. Arvas, IEEE Trans. Antennas Propagat. **44**, 1041 (1996).

*Corresponding author: ahsanilahi@gmail.com